Helical Superstructures and Related Spectral Changes of Bilayer Membranes of a Single-chain, Phosphate Amphiphile[1]

Toyoki Kunitake,* Jong-Mok Kim and Yuichi Ishikawa
Department of Organic Synthesis, Faculty of Engineering, Kyushu University, Fukuoka 812, Japan

The aggregation behaviour and spectroscopic properties of a single-chain phoshate amphiphile possessing a chiral centre and an azobenzene chromophore have been examined. At neutral and alkaline pH, the bilayer dispersion contained helical structures and red-shifted (bathochromic) absorptions and enhanced CD spectra were observed under the conditions where this helical structure was formed. These morphological and spectral changes are explained in terms of ordering and hydrogen-bonded interactions at the bilayer surface. Effects of amines and metal-ion salts are similarly explained; in particular the strong binding of Ca^{2+} ions is thought to be due to the ordering of the surface phosphate groups.

Synthetic bilayer membranes display physicochemical and functional characteristics that are similar to those of biolipid bilayer membranes.[2–4] The synthetic bilayer component can be selected from a large variety of the hydrophilic units, and novel bilayer compounds may be readily designed by combining a variety of hydrophobic and hydrophilic units.

Bilayer amphiphiles, both natural and synthetic, assume various aggregate morphologies such as vesicles, lamellae, rods, disks, tapes, tubes and helices, depending on the molecular structures and physical conditions of temperature, concentration, *etc.* In particular, chiral amphiphiles can form helical structures under appropriate conditions. We have briefly reported the formation of helical ribbons of double-chain ammonium amphiphiles.[5,6] Yamada *et al.*[7] simultaneously made a similar discovery. Fuhrhop and co-workers conducted a systematic study of the formation of helical fibres from *N*-alkylaldonamides.[8] The formation of helical tubules from phospholipids has been investigated by several groups.[9] Yanagawa *et al.*[10] have described the spontaneous formation of superhelical strands from a phospholipid-nucleoside conjugate.

In this study, we have synthesized the bilayer-forming phosphate amphiphile, C_{12}(L)AlaAzo$C_5PO_4H_2$ (**1**). This contains an alanine residue as a chiral centre and an azobenzene unit as a spectroscopic label. The azobenzene unit in bilayers of single-chain ammonium amphiphiles gives rise to large shifts in the absorption spectra which reflect the molecular orientation in the bilayer assembly.[11] In addition, the bilayer membranes of chiral amphiphiles often display remarkably enhanced circular dichroism,[12] which is sensitive to the mode of component alignment and the physical state of the membrane.[3] Owing to the presence of the two different 'labelling' groups, the aggregation behaviour of the new amphiphile can conveniently be studied by multiple physical techniques. We report here helix formation (see Fig. 1), its control by complexation with Ca^{2+}, and its relationship to the molecular orientation.

Experimental

Materials.—Dodecyl N-{4-[4-(5-*phosphopentyloxy*)*phenylazo*]*benzoyl*-L-*alaninate* [**1**; (C_{12}(L)AlaAzo$C_5PO_4H_2$]. 4-(4-Hydroxyphenylazo)benzoic acid was prepared by the procedure

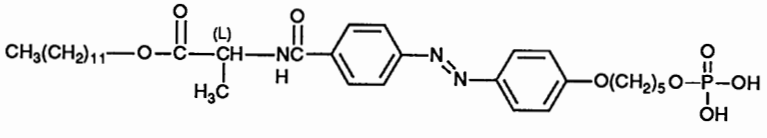

C_{12}AlaAzoC_5P (**1**)

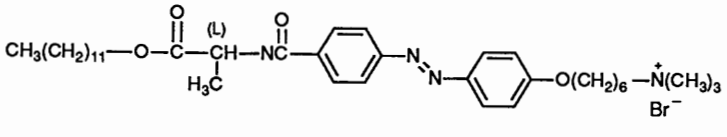

C_{12}AlaAzoC_6N^+ (**2**)

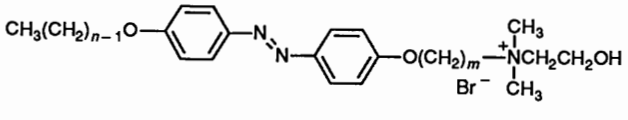

C_nAzo$C_m N^+$ (**3**)

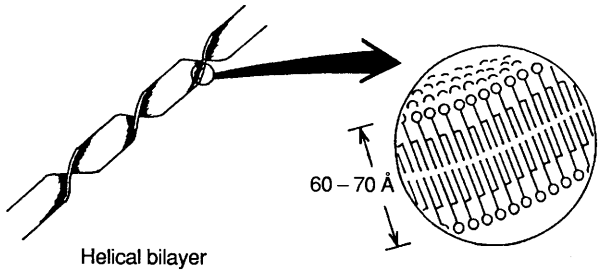

Fig. 1 Schematic representation of the helical bilayer

of Cohen and McGilbery,[13] m.p. 246→264 °C (decomp.) (the arrow indicates the liquid-crystalline range), (lit.,[13] m.p. 268 °C). The product (0.033 mol) and KOH (2 equiv.) were dissolved in ethanol and allowed to react with 5-bromopentan-1-ol (0.03 mol) in refluxing ethanol for 1 day to give 4-[4-(5-hydroxypentyloxy)phenylazo]benzoic acid in 57% yield; m.p. 185→226 °C (decomp.) (from acetic acid–ethyl acetate). ν_{max}(KBr)/cm^{-1} 1250 (C–O–C), 1680 (acid C=O), 2920 and 2859 (CH_2) and 3400 (OH).

The toluene-*p*-sulphonate salt of dodecyl-L-alaninate (0.006 mol) and triethylamine (0.007 mol) in dry tetrahydrofuran (THF) were added with stirring to a dry THF solution of the Williamson product (0.005 mol) and diethyl cyanophosphate (DECP) (0.01 mol) in an ice bath. After further stirring at room temperature for 2 days, $CHCl_3$ was added to the mixture, which was then washed with water and concentrated. The residue was recrystallized from hexane and subjected to column chromatography [Kieselgel 60 (70–230 mesh); eluent: $CHCl_3$–ethyl acetate (10:1 v/v)], to give dodecyl *N*-{4-[4-5-hydroxypentyloxy)phenylazo]benzoyl}-L-alaninate in 40% yield, m.p. 115→131 °C. ν_{max}(KBr)/cm^{-1} 1640 (amide C=O), 1740 (ester C=O) and 3440 (NH); δ($CDCl_3$) 0.9 (3 H, t, $-CH_3$), 1.1–2.5 (29 H, s + m, $-CH_2-$, CH_3), 3.4–4.3 (6 H, m, $-OCH_2-$), 5.4 (1 H, m, –CH–) and 7.2 and 7.9 (8 H, d, ArH) (Found: C, 69.0; H, 8.65; N, 7.2. Calc. for $C_{33}H_{49}N_3O_5 \cdot 0.5H_2O$: C, 68.72; H, 8.74; N, 7.29%).

This product (0.001 mol) and triethylamine (0.0012 mol) in dry tetrahydrofuran (THF) were added dropwise over 30 min, with stirring, to a dry THF solution of phosphorus oxychloride (0.01 mol) cooled in an ice bath. After 12 h of stirring at room temperature, cold water was added to decompose any unchanged $POCl_3$ until the mixture became cloudy, and the product was extracted with $CHCl_3$. Recrystallization of the product from $CHCl_3$–ethyl acetate (1:1 v/v) gave $C_{12}AlaAzoC_5PO_4H_2$ (**1**) in 32% yield as a yellow powder, m.p. 132→161 °C. ν_{max}(KBr)/cm^{-1} 1100 (P–O–C) (Found: C, 59.85; H, 7.8; N, 6.3. Calc. for $C_{33}H_{50}O_8N_3P \cdot H_2O$: C, 59.54; H, 7.87; N, 6.31%).

Experimental Measurements.—Electron microscopy was performed with a Hitachi H-600 instrument. Specimens were prepared by applying a drop of aqueous bilayer dispersions (1–2 mmol dm^{-3}) onto carbon-coated Cu grids, which were then negatively stained by the dropwise addition of 2% aqueous ammonium molybdate. Differential scanning calorimetry (DSC) was carried out for 20 mmol dm^{-3} samples with a Seiko Electronics SSC/560 instrument. The temperature was raised from 0 °C at a rate of 1 °C min^{-1}. The experimental details have been described elsehere.[14] For spectral measurements, 7–14 mg of the amphiphile were added to tris(hydroxymethyl)-aminomethane (Tris)–HCl buffer (pH 7.5, ionic strength 0.025) or to aqueous tetramethylammonium bromide (TMAB).

Samples of the mixture were sonicated for 30–60 s with a Bransonic Cell disruptor 185, to obtain clear dispersions (1–2 mM), which were then subjected to ageing for 10 min in ice–water and for 1 day at room temperature. These stock solutions were diluted with water or with Tris buffer when necessary. Absorption and circular dichroism spectra were obtained on a Hitachi 220A spectrophotometer and a JASCO J-40AS spectropolarimeter equipped with water-jacketed cell holders, respectively. Cells of path lengths of 1 cm and 1 mm were used.

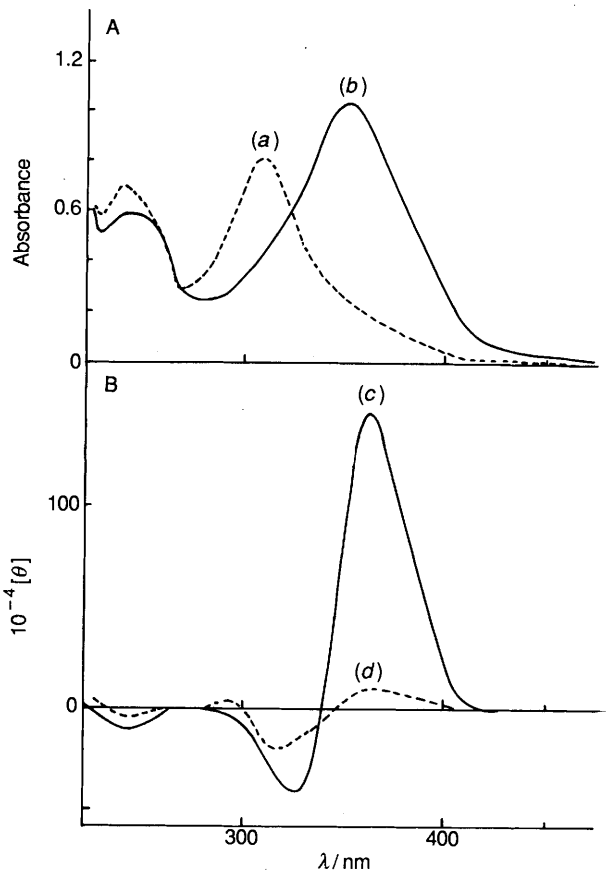

Fig. 2 Influence of pH on the absorption (A) and CD (B) spectra of the $C_{12}AlaAzoC_5PO_4H_2$ bilayer at pH = 7.5 (*b*, *c*) and pH = 9.6 (*a*, *d*). [$C_{12}AlaAzoC_5PO_4H_2$] = 4 × 10^{-5} mol dm^{-3}, T = 25 °C (below T_c), [TMAB] = 0.025 mol dm^{-3}, cell length = 1 cm, pH adjusted with 1 mol dm^{-3} NaOH. (*a*) λ = 310 nm; (*b*) λ = 355 nm; (*c*) [θ] = 140 × 10^{-4}; (*d*) 10 × 10^{-4}.

Results and Discussion

Formation of the Bilayer and its Superstructure.—The crystal-to-liquid-crystal phase transition is one of the most fundamental properties of bilayer membranes. A DSC thermogram of an aqueous dispersion (pH = 7.5, Tris buffer) of the phosphate amphiphile shows this transition as a broad endothermic peak at 92 °C (peak top) with ΔH = 29 kJ mol^{-1} and ΔS = 79 J K^{-1} mol^{-1}. An aqueous bilayer membrane of a structurally related ammonium amphiphile ($C_{12}AlaAzoC_6N^+$; **2**), gives a phase transition peak at 83 °C (ΔH = 38 kJ mol^{-1} and ΔS = 107 J K^{-1} mol^{-1}).[15] The polar interaction of the phosphate head group may raise the phase-transition temperature, relative to that of the ammonium bilayer.

Fig. 2 shows UV and CD spectra of the phosphate amphiphile dispersed in aqueous tetramethylammonium bromide (TMAB), with subsequent pH adjustment with 1 mol dm^{-3} NaOH. This amphiphile is not readily dispersed in aqueous inorganic salts; and, Tris buffers are therefore used, together with TMAB, which maintains a constant ionic strength. The absorption spectral data are quite different from those in ethanol (λ_{max} = 355 nm) in which the amphiphile is dispersed as individual molecules. At neutral pH,

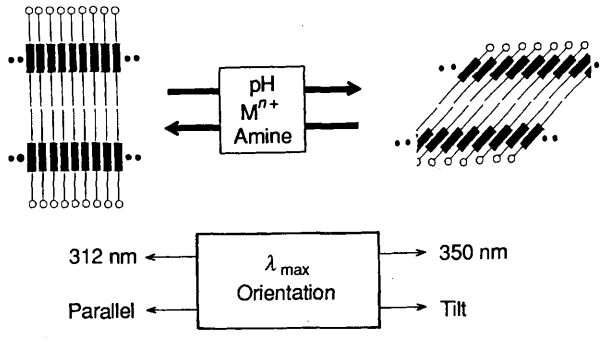

Fig. 3 Schematic representation of the orientational transformation of the phosphate bilayer

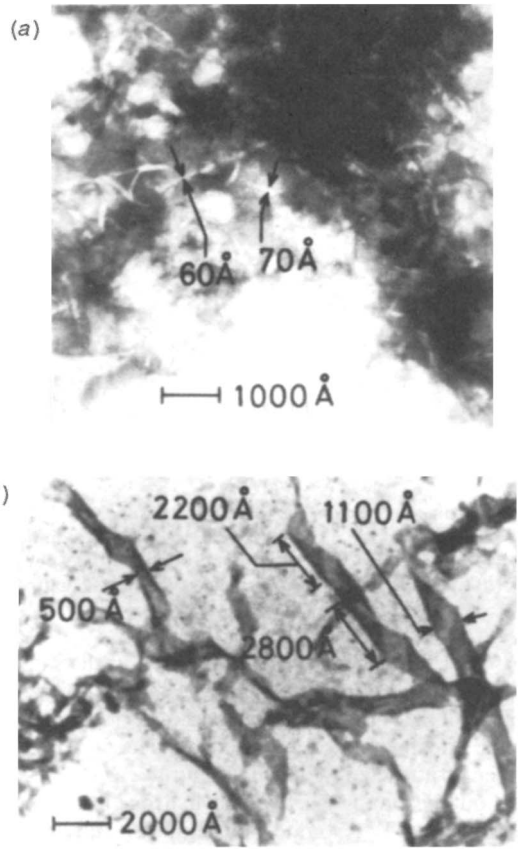

Fig. 4 pH dependence of the aggregate morphology of the $C_{12}AlaAzoC_5PO_4H_2$ bilayer as shown by electron microscopy. $[C_{12}AlaAzoC_5PO_4H_2]$ = 2 mmol dm^{-3}, pH adjusted with NaOH, room temperature, post-stained with 2% aqueous ammonium molybdate, acceleration voltage 75 kV. (*a*) at pH = 7 (NaOH), fibrous aggregate; (*b*) at pH = 10 (NaOH), helical aggregate.

λ_{max} is located at 310 nm, which shifts to 350 nm at the higher pH of 9.6. From pH 9.6 to 11.3 (the highest pH condition), the spectral pattern does not change, though the intensity decreases.

The absorption pattern of azobenzene-containing bilayers, **3**, in water shifts extensively owing to changing modes of chromophore stacking.[11] In the case of bilayer **3** (n = 8; m = 10), interdigitated molecular packing is found in which the azobenzene chromophore is in a parallel orientation and shows an extensive blue (hypsochromic) shift (λ_{max} = 300 nm) relative to its molecularly dispersed species (λ_{max} = 355 nm). In contrast, in the bilayer **3** (n = 12; m = 5) there is a tilted chromophore orientation which causes a large red shift (λ_{max} = 380 and 390 nm).

The observed pH dependence of the absorption spectra of the phosphate bilayer may be similarly explained by considering the change in molecular packing. The phosphate head group of **1** is mostly in the monoanionic form at neutral pH. A strong hydrogen-bonding interaction probably exists between the hydroxy and oxyanionic units at the bilayer surface, and the result is a parallel orientation with tight molecular packing. Increased dissociation of the phosphate group leads to loss of the hydrogen bonding and larger electrostatic repulsion among the head group. The enlarged surface of the phosphate head can be accommodated in the regular bilayer packing by tilting of the component molecule. This results in tilted chromophore packing and the consequent bathochromic shift. These situations are schematically illustrated in Fig. 3.

The CD spectra similarly display the characteristics peculiar to bilayer formation. The spectrum at pH 7.2 shows complex Cotton effects with $[\theta]_{325}$ of $-200\,000$ deg cm^2 $dmol^{-1}$ and $[\theta]_{360}$ of $+100\,000$. At pH 9.6, where the strongest CD intensity is observed, $[\theta]_{max}$ is enhanced to $+1.4 \times 10^6$ at 362 nm. The CD intensity decreases at still higher pH, $[\theta]_{362}$ being *ca.* $+10\,000$ at pH 11.3.

These CD intensities are much greater than that shown by the molecularly dispersed amphiphile in ethanol ($[\theta]$ = *ca.* 6000), and strongly suggest that the chromophores lie in a regular array. The CD enhancement in the alkaline pH region implies the formation of molecular organization of a high order.

This inference was supported by electron microscopy (Fig. 4). When the EM specimen is prepared from an aqueous dispersion at pH 7 (pH adjusted with NaOH), fibrous aggregates of diameter of 60–70 Å are found [Fig. 4(*a*)]. The extended molecular length of the phosphate amphiphile is estimated to be 40 Å from a CPK molecular model. Therefore, the fibres are presumably made of a tilted bilayer assemblage, although long-range structural regularity is not present. In contrast, helical superstructures are formed at pH 10, as in Fig. 4(*b*). The width of the twisted tapes is 200–1000 Å, and the helical pitch is 2000–3000 Å. The tape thickness is approximately 90 Å. Helix formation is not observed at pH 11.3, in agreement with the decreased $[\theta]$ value. Helices appeared again on lowering the pH of this solution to 10. This helical morphology is very similar to that observed for the bilayer of single-chain ammonium amphiphiles.[16]

Effect of Added Amines on Helix Formation.—The spectral characteristics of Fig. 1 become quite different when amines are added to the medium. λ_{max} of the aqueous phosphate bilayer is located at 350 nm at alkaline pH. This bathochromic shift becomes observable in the neutral pH region, if Tris buffer is used in place of NaOH to adjust pH; λ_{max} = 350 nm at pH 7.5, 0.025 mol dm^{-3} Tris–HCl, μ(TMAB) = 0.025, 20 °C. The CD spectrum of this sample is very similar, in both pattern and intensity, to that observed at pH 9.6 in Fig. 1: $[\theta]_{max}$ (361 nm) = 1.5×10^6. An electron microscopic observation indicates that helical tapes (width 1700 Å, pitch *ca.* 4000 Å) are formed under these conditions (Fig. 5).

These spectral and morphological changes appears to arise from the interaction of the phosphate head with the amine component. An aqueous dispersion of the phosphate bilayer (2×10^{-5} mol dm^{-3}), that is neutralized with NaOH, possesses λ_{max} at 306 nm, as shown in Fig. 2. When an equimolar amount of Tris is added to this dispersion, λ_{max} slowly shifts to 350 nm with an isosbestic point at 323 nm. The shift is complete within 1 h. Similar spectral shifts are observed when equimolar cyclam (1,4,8,11-tetraazocyclotetradecane) or ethylenediamine is added in place of Tris.

The observed bathochromic shifts can be associated with the change in molecular orientation. As mentioned above, partially dissociated phosphate groups in the neutral pH region would be tightly packed owing to hydrogen bonding. Protonated amines would be inserted in the hydrogen-bond network at the bilayer

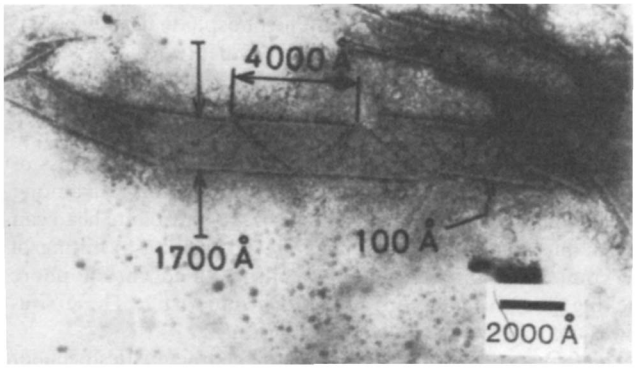

Fig. 5 Electron micrograph of the $C_{12}AlaAzoC_5PO_4H_2$ bilayer pH = 7.5 (Tris–HCl buffer, 1 mmol dm^{-3}. The other conditions are the same as those in Fig. 4.

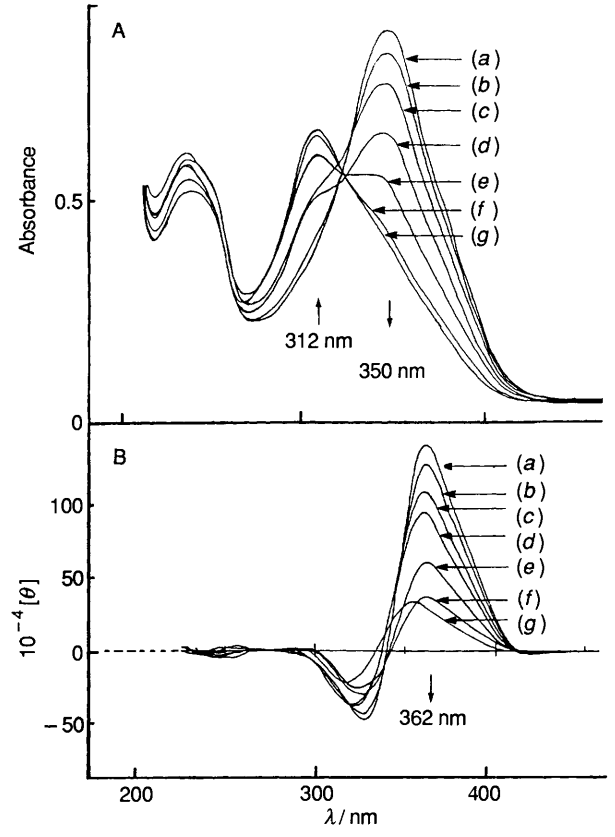

Fig. 6 Influence of added Ca^{2+} ion on absorption (A) and CD (B) spectra of the $C_{12}AlaAzoC_5PO_4H_2$ bilayer. $[C_{12}AlaAzoC_5PO_4H_2]$ = 4×10^{-5} mol dm^{-3}, $[CaCl_2]$ = (0.4–4.0) $\times 10^{-5}$ mol dm^{-3}, 25 °C (below T_c), Tris–HCl buffer [pH = 7.5; 0.025 mol dm^{-3}, μ = 0.025 (TMAB)]; ageing: 2 days after addition of $CaCl_2$ at room temperature; cell length = 1 cm. $[CaCl_2]$/[Bilayer] = (*a*) 0; (*b*) 0.1; (*c*) 0.2; (*d*) 0.3; (*e*) 0.5; (*f*) 0.75; (*g*) 1.0.

surface by replacing non-hydrogen-bonding counter-cations, and increase the apparent surface area per phosphate. This would lead to tilting of the hydrophobic chain in order to maintain the molecular packing observable by the bathochromic shift of the azobenzene absorption.

Effect of Alkali-metal Ions on Molecular Orientation.—The spectral properties, and therefore the molecular orientation, of the phosphate bilayer is extensively altered by added metal ions. When 0.025 mol dm^{-3} alkali-metal salts are added to an aqueous dispersion of the phosphate bilayer in 0.02 mol dm^{-3} Tris–HCl buffer (pH 7.5) at 20 °C, λ_{max} at 350 is suppressed with the concomitant appearance of a new peak at 310 nm. The salt effect is intensified in the order of TMAB ~ LiCl < NaCl < CsCl. The CD intensity is lowered in the same order. These salt effects are interpreted as the salt counteracting the effect of the Tris buffer, which increases the apparent surface area of the phosphate head by insertion. The alkali-metal ions would then be attracted to the bilayer surface as simple counter-ions without becoming part of the hydrogen-bond network. Expulsion of the Tris counter-ion should result in a tighter packing of the phosphate. The ease of replacement of Tris–HCl should follow the decreasing order of hydration of metal ions: $Cs^+ > Na^+ > Li^+$.

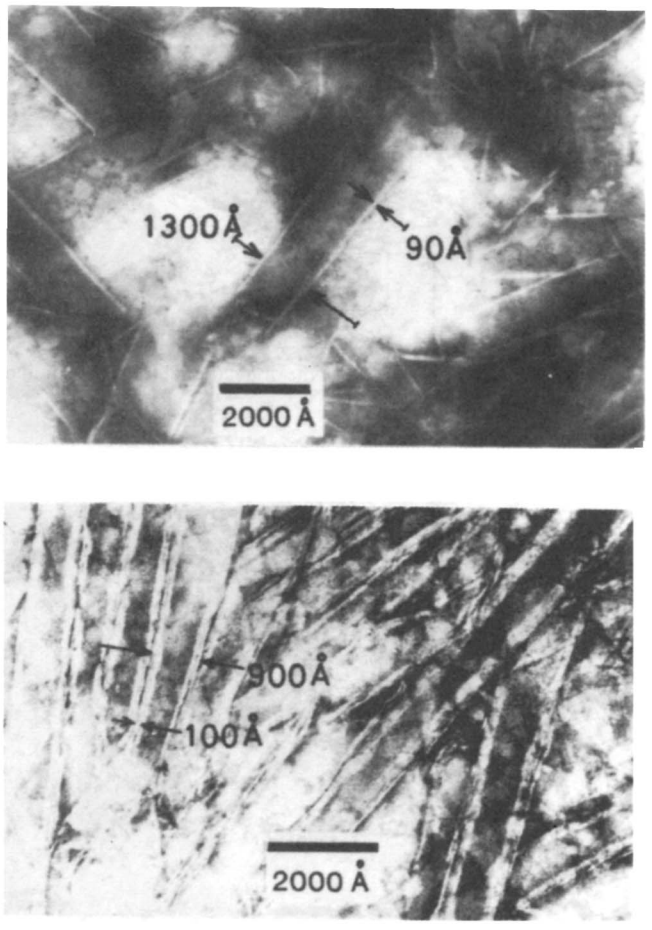

Fig. 7 Electron micrographs of the $C_{12}AlaAzoC_5PO_4H_2$ bilayer in the presence of $CaCl_2$. $[C_{12}AlaAzoC_5PO_4H_2]$ = 2 mmol dm^{-3}, $[CaCl_2]$ = 1 mmol dm^{-3}. The other conditions are the same as those of Fig. 4. (*a*) tube-like structures; (*b*) rugged tube-like structures.

Influence of Ca^{2+} *on Molecular Orientation.*—The effect of metal salts is greater in the case of multivalent metal ions. We describe here the effect of $CaCl_2$ as a representative case. Fig. 6 displays UV and CD spectral changes of the phosphate bilayer upon addition of $CaCl_2$ up to the stoichiometric amount. Addition of more than equimolar $CaCl_2$ caused precipitation of equimolar Ca^{2+}–bilayer complexes in which the bilayer assembly is preserved. This complex can be dispersed in some organic media without losing the ordered, two-dimensional structure.[17]

The spectra were measured two days after each addition of $CaCl_2$, in order to ensure structural equilibration. The effect of $CaCl_2$ on the spectra is similar to those of alkali-metal ions, although it was observed at much lower concentrations. Added $CaCl_2$ produces a new peak at 312 nm at the expense of the original peak at 350 nm. The much enhanced CD spectrum is correspondingly suppressed by progressive addition of $CaCl_2$. The explanation accounting for the alkali-metal salt effect also

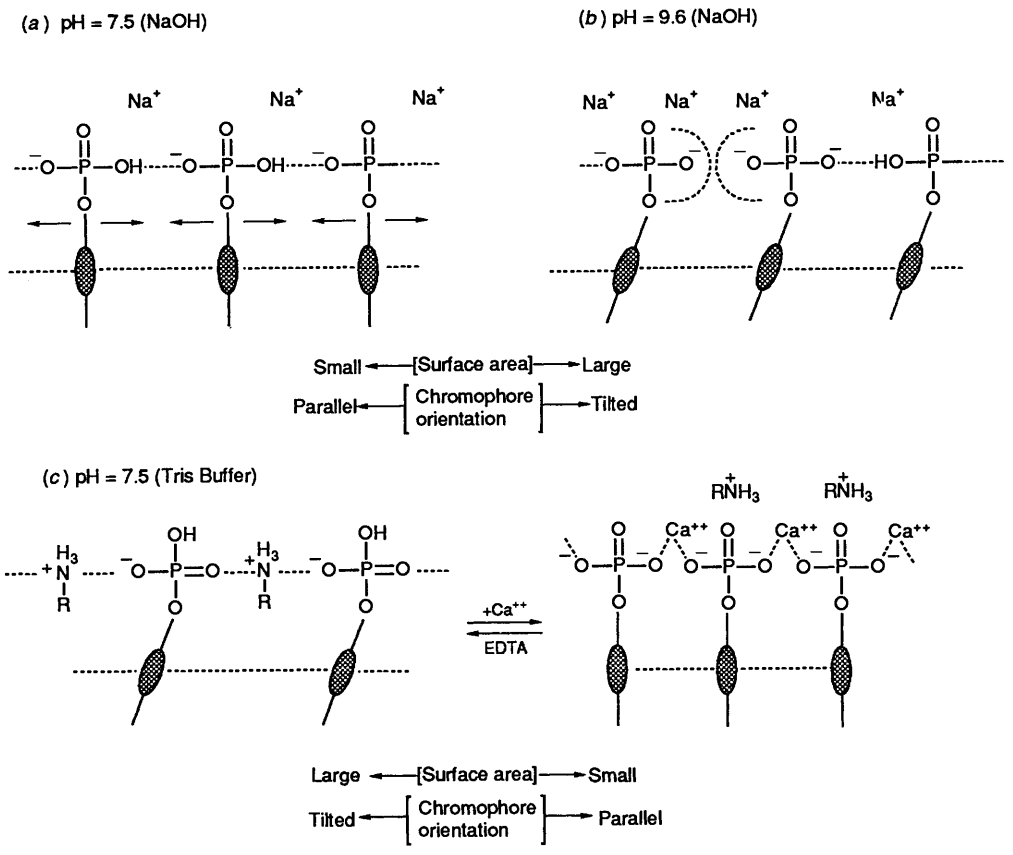

Fig. 8 Schematic representations of the relationship between the chromophore orientation and the surface structure in the phosphate bilayer. (*a*) pH = 7.5 adjusted with NaOH. Attractive hydrogen bonding interaction among the monoanionic phosphate heads. (*b*) pH = 9.6 adjusted with NaOH. Coexistence of repulsive interactions among the dianionic phosphate (−2) heads and attractive interaction as in (*a*). (*c*) pH = 7.5 adjusted with Tris–HCl buffer. Interaction of the phosphate head group with protonated amines and Ca^{2+}.

explains these spectral changes: Ca^{2+} ion replaces Tris–HCl which is involved in the hydrogen-bond network at the membrane surface. The replacement results in more compact surface areas which favour parallel chromophore orientation with a hypsochromically shifted absorption and low CD intensity. The original UV and CD spectra are regenerated by addition of ethylenediaminetetraacetic acid.

Electron microscopy of the aqueous dispersion (in Tris buffer) which additionally contains 0.5 equiv. $CaCl_2$ shows the presence of large neat tubes [Fig. 7(*a*)]and rugged multilamellar tubes [Fig. 7(*b*)], but helical aggregates are not found. The original dispersion (without $CaCl_2$) contained helical tapes as shown in Fig. 4. The rigid tube in Fig. 7(*a*) has a diameter of 1300–1600 Å and a wall thickness of 80–100 Å. The tubular structure is multi-walled and less regular in Fig. 7(*b*). (Only a part of the total structure is shown in this EM picture.)

By using the spectral data of Fig. 6, we can estimate the value of the stability constant K, from the following relationships.[18]

$$M^{2+} + L \overset{K}{\rightleftharpoons} M^{2+}\cdot L \quad (1)$$

$$K = [M^{2+}L]/([M^{2+}][L]) \quad (2)$$

For UV data, eqn. (3) holds, where A_J and A_H are

$$\log [(A_J - A)/(A - A_H)] = \log [Ca^{2+}] + \log K \quad (3)$$

absorbances at 350 nm for the bilayer in the absence of Ca^{2+} and for the fully complexed (and aged) bilayer, respectively, and A is the absorbance at 350 nm in the presence of given amounts of Ca^{2+}.

For CD data, eqn. (4) is valid, where $[\theta]_J$ and $[\theta]_H$ are

$$\log \{([\theta]_J - [\theta])/([\theta] - [\theta]_H)\} = \log [Ca^{2+}] + \log K \quad (4)$$

CD intensities at 362 nm of the phosphate bilayer under the conditions corresponding to A_J and A_H in (3), respectively.

The plots of the left-hand side of eqns. (3) and (4) against $\log [Ca^{2+}]$ gave satisfactorily linear relationships, and the stability constant K was estimated to be $10^{7.5}$ dm^3 mol^{-1} from the UV data and $10^{7.6}$ dm^3 mol^{-1} from the CD data. The agreement between the two sets of data is remarkable.

This stability constant with Ca^{2+} is greater, by a factor of 10^3–10^6, than those of the mono-, di- and tri-dentate ligands: aminomethylphosphonic acid ($K = 10^{1.84}$ dm^3 mol^{-1}),[19] iminodiacetic acid ($K = 10^{2.59}$ dm^3 mol^{-1})[20] and methylenediphosphonic acid ($K = 10^{4.70}$ dm^3 mol^{-1}).[19] However, it is smaller than those of the hexadentate ligands by a factor of 10^3–10^{10}: ethylenedamine-*N*,*N*,*N*′,*N*′-tetrakismethylenephosphoric acid ($K = 10^{16.53}$ dm^3 mol^{-1})[20] and EDTA ($K = 10^{10.96}$ dm^3 mol^{-1}).[20]

The component molecule of the phosphate bilayer is a monodentate, but the stability constant of the bilayer is greater than those of the mono-, di and tri-dentate ligands. This enhanced binding is produced by the two-dimensional ordering of the phosphate unit at the bilayer surface. However, that of the bilayer is smaller than those of the typical hexadentate chelates. The planar arrangement of the ligand in the bilayer would not be suitable to produce octahedral phosphate co-ordination with Ca^{2+}.

Conclusions

It is clear that the aggregate morphology (*i.e.* the formation of the helical superstructure) and the component alignment of the phosphate bilayer are both affected by the mode of interaction of the head groups. As shown in Fig. 8, strong phosphate interactions are expected for a dispersion neutralized with NaOH. The phosphate interaction is weakened upon further neutralization owing to enhanced Coulombic repulsion and loss of hydrogen-bonding interaction. Insertion of protonated amines at neutral pH separates the neighbouring phosphate heads, but replacement of protonated amines by metal ions brings them together. The enlarged surface area per molecule is associated with helix formation, tilted alignment of the chromophore and enhanced CD intensity.

This unified understanding of the relationship between the component orientation and the head-group interaction should prove useful in the development of novel functions for phosphate bilayer membranes.

Strengthened binding of metal ions due to ordering of the phosphate unit is also useful for this purpose. Some years ago, we showed that enhanced CD intensity of a chiral, double-chain phosphate bilayer is drastically suppressed by the addition of metal ions. We suggested that this constituted a sensitive detection system for metal ions.[12] The present result reinforces this proposition.

It is well known that the physiological properties of biomembranes, such as membrane fusion and phase separation, are altered by the head-group interactions of phospholipid components with Ca^{2+} and other small molecules. The pattern of interaction of the phosphate group described in this study may well be related to functional control in biomembranes.

References

1 Contribution No. 931 from the Department of Organic Synthesis, Faculty of Engineering, Kyushu University.
2 J. H. Fendler, *Membrane Mimetic Chemistry*, Wiley-Interscience, New York, 1982, ch. 6.
3 H. Ringsdorf, B. Schlarb and J. Venzmer, *Angew. Chem., Int. Ed. Engl.*, 1988, **27**, 113.
4 T. Kunitake, *Angew. Chem., Int. Ed. Engl.*, in press.
5 N. Nakashima, S. Asakuma and T. Kunitake, *Chem. Lett.*, 1984, 1709.
6 N. Nakashima, S. Asakuma and T. Kunitake, *J. Am. Chem. Soc.*, 1985, **107**, 509.
7 K. Yamada, H. Ihara, T. Ide and T. Fukumoto, *Chem. Lett.*, 1984, 1713.
8 *E.g.*, J.-H. Führhop, S. Svenson, C. Boettcher, E. Rossler and H.-M. Vieth, *J. Am. Chem. Soc.*, 1990, **112**, 4307.
9 *E.g.*, J. H. Georger, A. Singh, R. R. Price, J. M. Schnur, P. Yager and P. E. Schoen, *J. Am. Chem. Soc.*, 1987, **109**, 6169.
10 H. Yanagawa, Y. Ogawa, H. Furuta and K. Tsuno, *J. Am. Chem. Soc.*, 1989, **111**, 4567.
11 M. Shimomura, R. Ando and T. Kunitake, *Ber. Bunsenges. Phys. Chem.*, 1983, **87**, 1134.
12 N. Nakashima, R. Ando, H. Fukushima and T. Kunitake, *Chem. Lett.*, 1985, 1503.
13 P. P. Cohen and R. W. McGilvery, *J. Biol. Chem.*, 1946, **166**, 261.
14 J.-M. Kim and T. Kunitake, *Mem. Fac. Eng. Kyushu Univ.*, 1989, **49**, 93.
15 T. Kunitake, R. Ando and Y. Ishikawa, *Mem. Fac. Eng. Kyushu Univ.*, 1986, **46**, 245.
16 T. Kunitake and N. Yamada, *J. Chem. Soc., Chem. Commun.*, 1986, 655; Y. Ishikawa, T. Nishimi and T. Kunitake, *Chem Lett.*, 1990, 25.
17 J.-M. Kim and T. Kunitake, *Chem. Lett.*, 1989, 959.
18 For example, Y. Murakami, Y. Hisaeda and A. Kajihara, *Bull. Chem. Soc. Jpn.*, 1983, **56**, 3642; D. P. Rillema, C. M. Wicker, Jr., R. D. Morgan, L. F. Barringer and L. A. Scism, *J. Am. Chem. Soc.*, 1982, **104**, 1276.
19 Compiled by Douglas D. Perrin, *Stability Constants of Metal-ion Complexes: Part B (Organic Ligands)*, Pergamon Press, 1979.
20 *Catalog of the Dojindo Lab. (Japan)*, 16th edn., 1990, p. 137.

Paper 0/04744I
Received 22*nd October* 1990
Accepted 17*th January* 1991